JOURNAL OF VIROLOGY, Oct. 1995, p. 6259–6264 Vol. 69, No. 10
0022-538X/95/$04.00+0

In Vivo Pathogenic Properties of Two Clonal Human Immunodeficiency Virus Type 1 Isolates

BETH D. JAMIESON,[1] SHEN PANG,[2] GRACE M. ALDROVANDI,[1]
JUNLI ZHA,[1] AND JEROME A. ZACK[1]*

Division of Hematology-Oncology Department of Medicine,[1] and Division of Urology, Department of Surgery,[2] UCLA School of Medicine, Los Angeles, California 90095

Received 12 April 1995/Accepted 10 July 1995

We have investigated the in vivo pathogenic properties of two molecularly cloned strains of human immunodeficiency virus type 1 (HIV-1), HIV-1_{NL4-3} and HIV-1_{JR-CSF}, in human fetal thymus/liver implants in severe combined immunodeficient mice. Studies comparing their in vivo replication kinetics and abilities to induce $CD4^+$ thymocyte depletion were performed. HIV-1_{NL4-3} replicated in vivo with faster kinetics and induced greater levels of $CD4^+$ thymocyte depletion than did HIV-1_{JR-CSF}. These results demonstrate that different viral isolates have different pathogenic properties in this system. In the SCID-hu model, this pathogenesis most likely occurs in the absence of an immune response. Therefore, we investigated whether the absence of immune selection resulted in extensive genetic variation and the generation of viral quasispecies. To this end, DNA corresponding to the fourth variable domain region of the viral envelope gp120 protein recovered from biopsy samples at 6 weeks postinfection was sequenced. Little genetic variation was noted in either HIV-1_{JR-CSF}- or HIV-1_{NL4-3}-infected implants. The mutation levels demonstrated in both viral strains were more reflective of the acute rather than the chronic phase of HIV-1 infection in humans. These results suggest that the SCID-hu mouse model can be used to study the in vivo pathogenicity of different HIV-1 isolates in the absence of host immune selective pressures.

The biological properties of human immunodeficiency virus type 1 (HIV-1) that influence its pathogenicity are poorly understood but are of critical importance to the development of both vaccines and therapeutic strategies. Viral burden and syncytium induction have both been proposed as important factors in the destruction of the immune system and induction of disease (7–10, 25, 26, 28). Longitudinal studies of HIV-infected individuals have revealed that a decline in $CD4^+$ T-cell numbers occurs in the peripheral blood in conjunction with an increase in viral burden (7, 9, 28). However, not all studies find a correlation between a switch to a syncytium-inducing (SI) phenotype and the decline of $CD4^+$ T-cells, leaving the role of syncytium induction in in vivo pathogenesis unclear (9, 14). In addition, it is unclear whether the decline in $CD4^+$ T cells is a result of the emergence of SI isolates or whether the loss of immune surveillance allows for the emergence of this viral phenotype.

The SCID-hu mouse (20) is a small animal model for HIV-1 pathogenesis. It employs severe combined immunodeficient (SCID) mice that are T- and B-cell deficient and therefore incapable of rejecting xenografts. Implantation of human fetal thymus and liver under the kidney capsule results in formation of a conjoint organ (Thy/Liv) capable of supporting the differentiation and maturation of human thymocytes for up to 1 year (22). The Thy/Liv implant histologically resembles a normal human thymus (2, 4, 19, 22, 30). Direct infection of the Thy/Liv implant with HIV-1 results in hypocellularity (2, 4, 30), loss of cortical-medullary junctions, and depletion of CD4-bearing cells (2, 4), similar to what is seen in HIV-infected humans. We have used this model to examine the pathogenic potential of prototypes of non-SI (NSI) and SI isolates of HIV-1 with respect to their replication capacities and $CD4^+$ cell decline. To determine the extent of viral variation that occurs in the SCID-hu mouse, DNA corresponding to the fourth variable domain (V4) region of the *env* gene of provirus was recovered from infected implants and sequenced. Our results indicate that a molecular clone of HIV-1 which has an SI phenotype (HIV-1_{NL4-3}) replicated to higher titer and resulted in more severe depletion of $CD4^+$ cells than a molecular clone of NSI phenotype (HIV-1_{JR-CSF}). In addition, strikingly little *env* sequence variation was observed throughout the course of infection, consistent with the lack of immune selection in this system. Thus, it appears that the SCID-hu mouse is an important system for evaluating the innate pathogenic potential of various viral strains in the absence of host-derived immune factors.

MATERIALS AND METHODS

Construction of SCID-hu mice. C.B.-17 mice homozygous for the SCID genetic defect (5) were bred at the University of California, Los Angeles, housed in a biosafety level 3 animal facility, and maintained free of antibiotics. SCID-hu mice were constructed as previously described (2, 4, 12, 20, 22). Briefly, human fetal thymus (≈1 mm^2) was sandwiched between two pieces (≈1 mm^2) of human fetal liver from the same donor and implanted under the left kidney capsule of SCID mice. Fetal tissue purchased from Advanced Bioscience Resources (Alameda, Calif.) was obtained from fetuses ranging in gestational age from 16 to 24 weeks. Trimethoprim (16 mg/ml)-sulfamethoxazole (80 mg/ml) was administered in drinking water for 3 days per week to experimental animals as a prophylaxis for *Pneumocystis carinii*. Four to eight months postimplantation, implants were injected with 100 infectious units (IU) of HIV-1_{NL4-3} (1) or HIV-1_{JR-CSF} (17) in 50-μl volumes (2, 12). In the data presented in the figures and tables, the animals are identified by numbers. The number preceding the hyphen indicates the fetal tissue donor, and the number after the hyphen represents the particular mouse in that transplantation series.

Preparation of virus stocks and infection of SCID-hu mice. HIV-1_{JR-CSF} (17) and HIV-1_{NL4-3} (1) have been previously described. Virus stocks were obtained by electroporation (6) of infectious cloned proviral DNA (50 μg) into 10^7 mycoplasma-free COS cells. Virus stocks were collected 1, 2, and 3 days posttransfection and analyzed for $p24^{gag}$ content by enzyme-linked immunosorbent assay (Coulter, Hialeah, Fla.). Virus stocks were stored at −70°C. Infectious units were

* Corresponding author. Mailing address: Division of Hematology-Oncology, 11-934 Factor Bldg., Department of Medicine, UCLA School of Medicine, Los Angeles, CA 90095-1678. Phone: (310) 794-7765. Fax: (310) 825-6192.

TABLE 1. Thymocyte subset distribution of HIV-1_{JR-CSF}- and HIV-1_{NL4-3}-infected implants[a]

Infection	3 wk p.i.					4–6 wk p.i.				
	%				No. showing depletion/ total	%				No. showing depletion/ total
	$CD4^+$	$CD4^+$ $CD8^+$	$CD4^-$ $CD8^-$	$CD8^+$		$CD4^+$	$CD4^+$ $CD8^+$	$CD4^-$ $CD8^-$	$CD8^+$	
Mock	17.8 ± 11.0	72.3 ± 16.5	2.8 ± 2.0	7.0 ± 6.6	0/11	17.3 ± 8.4	68.3 ± 13.0	6.3 ± 6.3	8.0 ± 6.1	0/11
HIV-1_{JR-CSF}	24.1 ± 13.1	65.0 ± 14.4	2.4 ± 1.1	6.8 ± 4.8	0/10	19.6 ± 11.3	65.9 ± 13.5	4.5 ± 3.7	8.3 ± 3.7	2/12
HIV-1_{NL4-3}	16.2 ± 11.4	63.6 ± 28.9	4.0 ± 5.7	14.2 ± 15.1	2/10	15.8 ± 13.9	10.9 ± 26.4	45.2 ± 29.4	27.4 ± 23.6	12/12

[a] Implants infected as indicated were analyzed by flow cytometry for CD4 and CD8 surface markers. Mock-infected implants were assayed in parallel with HIV-infected implants at each time point. Quadrants were set by using the mock-infected implants. Values are the averages of 10 to 12 implants per group ± standard deviation. Depletion was scored as positive if CD4 CD8 double-positive thymocytes fell below 51% of the gated population.

determined for each virus stock by limiting dilution analysis using normal human peripheral blood mononuclear cells (PBMC) previously stimulated for 3 days with phytohemagglutinin. Leukopacks purchased from the American Red Cross served as the source of normal human PBMC. Thy/Liv implants were infected with 100 IU by direct injection of 50 to 100 μl of virus. Mock implants were infected with 50 to 100 μl of supernatant from mock-electroporated COS cells. Sequential wedge biopsies of approximately 25% of each implant were obtained at the indicated times while the animals were sedated. Because of the large number of animals needed, data presented were obtained from three independent experiments comparing infection with the two viral strains in parallel. The first biopsy was performed 3 weeks postinfection (p.i.), and the second was performed 4 to 6 weeks p.i. Data obtained were consistent in all three experiments.

Flow cytometry. To determine thymocyte subset distribution in infected and mock-infected implants, single-cell suspensions obtained from biopsy samples were washed once in phosphate-buffered saline (PBS), and then 10^6 cells were costained with monoclonal antibodies (MAbs) (Becton Dickinson, Mountain View, Calif.) against CD4 and CD8 T-cell markers. Anti-CD4 and anti-CD8 MAbs were directly conjugated to fluorescein isothiocyanate and phycoerythrin, respectively. As a positive control, normal human peripheral blood was stained with anti-CD4 and anti-CD8 MAbs. At all time points, anti-mouse immunoglobulin G1 MAbs (Becton Dickinson), both fluorescein isothiocyanate and phycoerythrin conjugated, were used as an antibody isotype control. After staining, erythrocytes were lysed by incubation in fluorescence-activated cell sorting lysing solution (Becton Dickinson). Cells were then fixed in 2% paraformaldehyde. Data were accumulated on a FACStar^{plus} flow cytometer and analyzed with the Lysis II program (Becton Dickinson). Forward versus side scatter analysis of mock-infected implants was used to gate on the live thymocyte population. A total of 5×10^3 to 10×10^3 events were acquired, except from implants severely depleted of CD4-bearing thymocytes.

Quantitative PCR. Single-cell suspensions obtained from biopsy samples were washed once in PBS and then lysed in urea lysis buffer (4.7 M urea, 1.3% [wt/vol] sodium dodecyl sulfate, 0.23 M NaCl, 0.67 mM EDTA [pH 8.0], 6.7 mM Tris-HCl) and subjected to phenol-chloroform extraction and ethanol precipitation. Total nucleic acids obtained from this procedure were then subjected to quantitative PCR as previously described (2, 34, 35). Briefly, HIV DNA was detected by using the ^{32}P-end-labeled M667-AA55 primer pair specific for the R/U5 region of the long terminal repeat. Twenty-five cycles of amplification were used. Standard curves for HIV-1 DNA were generated by using four- or fivefold dilutions of cloned HIV-1_{JR-CSF} DNA linearized with *Eco*RI, which does not digest viral sequences. The dilutions were made into DNA from normal human PBMC (10 μg/ml). To quantitate HIV genomes per human cell, replicate samples were analyzed for human DNA with primers specific for nucleotides (nt) 14 to 33 and 123 to 104 of the human β-globin gene (18, 34), using 21 cycles of amplification. Standard curves for human β-globin were generated from 3- and 10-fold dilutions of PBMC DNA, and values were obtained by interpolation from the standard curve, using an Ambis (San Diego, Calif.) radioanalytic imager.

Cloning and sequencing of the V4 envelope region. HIV-1_{JR-CSF} *env* present in Thy/Liv implants was amplified, cloned, and sequenced as previously described (24). A modified version of that protocol was used to amplify, clone, and sequence the corresponding *env* region from HIV-1_{NL4-3}-infected implants. Briefly, nested PCR of the *env* V4 region was performed with the *env* 5′ primer (5′-CAGATAGTTGAAAAATTAAGA-3′ [sense]; nt 7256 to 7276 of HIV-1_{JR-CSF}) and the *env* 3′ primer (3′-ATAATTCACTTCTCCAATTGT-5′ [antisense]; nt 7661 to 7641 of HIV-1_{JR-CSF}) as the outside primer pair. Samples were amplified in 50-μl volumes for 35 cycles of denaturation at 94°C for 1 min, annealing at 55°C for 1 min, and extension at 72°C for 2 min. After the first round of amplification, nested PCR was performed by removing 10 μl of sample and adding this to 45 μl of fresh PCR reagents containing env 21 and env 22 primers (24) as the internal primer pair. Amplification conditions were identical to those for the previous 35 cycles. An *Eco*RI site and a *Bam*HI site were included on env 22 and env 21 primers, respectively, and used for ligation of the amplified products into *Escherichia coli* XL1-Blue MRF′ (Stratagene, La Jolla, Calif.). White colonies were screened by digestion of the DNA at the *Eco*RI and *Bam*HI restriction sites, and the products were separated on a 1% agarose gel. DNA from positive colonies was sequenced by the method of Sanger et al. (27), using a Sequenase version 2.0 kit (U.S. Biochemical, Cleveland, Ohio).

RESULTS

Pathogenic properties of HIV-1 strains in vivo. To investigate the in vivo cytopathicity of HIV-1_{NL4-3} and HIV-1_{JR-CSF}, Thy/Liv implants were mock infected or infected with 100 IU of virus. At 3 and at 4 to 6 weeks p.i., implants from all three groups were biopsied. Thymocyte subset distribution was determined by anti-CD4 and anti-CD8 fluorescent-antibody staining followed by flow cytometric analysis. No thymocyte depletion was seen in 10 implants infected with HIV-1_{JR-CSF} at 3 weeks p.i. (Table 1). At later time points, depletion was observed in two of the 12 HIV-1_{JR-CSF}-infected implants. In contrast, at 3 weeks p.i., 2 of 10 HIV-1_{NL4-3}-infected implants showed depletion of both CD4 CD8 double-positive and $CD4^+$ $CD8^-$ subsets. By 4 to 6 weeks p.i., severe depletion of all CD4-bearing thymocyte subsets was demonstrated in 12 of 12 HIV-1_{NL4-3}-infected implants. These data clearly demonstrate that HIV-1_{NL4-3} is more cytopathic in vivo, depleting CD4-bearing thymocytes more rapidly than did HIV-1_{JR-CSF}.

In vivo replication kinetics of HIV-1_{NL4-3} and HIV-1_{JR-CSF}. Previous experiments (12) indicated that HIV-1_{NL4-3} may replicate to higher titers in vivo in Thy/Liv implants than does HIV-1_{JR-CSF}. To investigate the kinetics of viral replication, single-cell suspensions obtained from biopsy samples of implants infected with either virus were analyzed by quantitative PCR as previously described (2, 12, 34, 35). Figure 1A shows virus load in HIV-1_{NL4-3}- and HIV-1_{JR-CSF}-infected implants at 3 and at 4 to 6 weeks p.i. HIV-1_{NL4-3} displayed more rapid replication kinetics than HIV-1_{JR-CSF}, reaching an ≈11-fold higher titer at 3 weeks p.i. (Table 2). At 4 to 6 weeks p.i., viral burden in HIV-1_{NL4-3}-infected implants remained relatively constant, with ≈13,200 copies of HIV-1 DNA per 10^5 cells. Virus load in HIV-1_{JR-CSF}-infected implants increased by ≈2-fold (Table 2) but remained ≈5-fold lower than in HIV-1_{NL4-3}-infected implants.

As previously reported (2), proviral load drops somewhat when severe depletion of CD4-bearing cells is observed. Because $CD4^+$ cells are the primary cell type in which HIV-1 DNA is found in the SCID-hu mouse (2), the depletion of $CD4^+$ thymocytes would be expected to affect the overall viral burden in the implant. A comparison between implants infected with HIV-1_{NL4-3}, which are severely depleted of CD4-bearing cells, and HIV-1_{JR-CSF}-infected implants, which are not depleted, becomes difficult to interpret. Therefore, viral burden per 10^5 $CD4^+$ cells was calculated by quantitative PCR

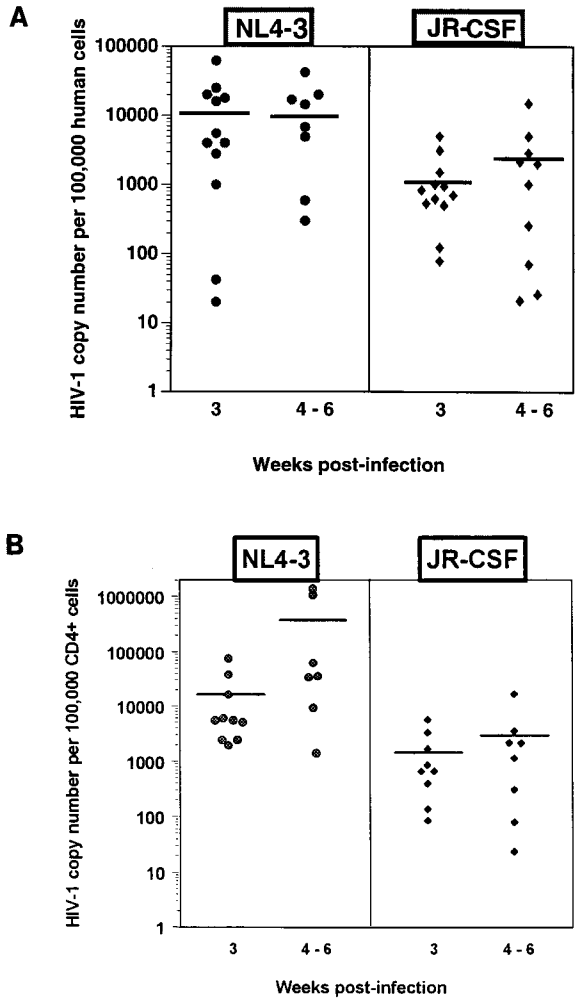

FIG. 1. In vivo replication of HIV-1_{NL4-3} and HIV-1_{JR-CSF}. The number of HIV-1 genomes per 10^5 human thymocytes (A) or per 10^5 $CD4^+$ thymocytes (B) was determined by quantitative PCR of sequential biopsy samples from Thy/Liv implants. Replicate samples were analyzed for both HIV-1 genomes and human β-globin sequences to allow quantitation of viral genomes per human cell equivalent. The number of $CD4^+$ thymocytes present per sample was determined by anti-CD4 staining followed by flow cytometry. Each symbol represents virus load in an individual implant.

for viral sequences and by two-color flow cytometric analysis for CD4 and CD8 surface markers. As indicated in Fig. 1B, when the relative number of HIV-1 genomes is calculated per $CD4^+$ thymocyte, the results are even more striking. HIV-1_{NL4-3}-infected implants still demonstrate ≈11-fold-higher viral burden at the 3-week time point than HIV-1_{JR-CSF}-infected implants, since little $CD4^+$ thymocyte depletion was observed at this time point (Table 2). However, at 4 to 6 weeks p.i., when HIV-1_{NL4-3}-infected implants had become severely depleted of $CD4^+$ cells, the calculated viral burden per $CD4^+$ cell in those implants was ≈23-fold higher than at the 3-week time point (Table 2). This is equivalent to an ≈112-fold-greater calculated viral burden than was achieved in implants infected with HIV-1_{JR-CSF}. These results clearly demonstrate that HIV-1_{NL4-3} replicates more rapidly in vivo in the SCID-hu mouse than does HIV-1_{JR-CSF}. Our previous studies (2, 12) suggested that high virus load (5 to 50% of thymocytes infected) was required prior to depletion of thymocytes. Our current results suggest that the differences in replication rates between HIV-1_{NL4-3} and HIV-1_{JR-CSF} in the implants may at least partially contribute to the differences in pathogenic properties.

Genetic variation in vivo. We next examined whether significant viral genetic variation occurred in the Thy/Liv implants. To this end, the *env* gene region coding for the V4 region and the CD4-binding region of gp120 was PCR amplified, cloned, and sequenced from HIV-1_{NL4-3}- and HIV-1_{JR-CSF}-infected biopsy samples. Of the 30 clones derived from two HIV-1_{JR-CSF}-infected implants at 6 weeks p.i., only one nucleotide change was observed (Fig. 2A). Of the 18 clones obtained from three HIV-1_{NL4-3}-infected implants at 6 weeks p.i., 7 contained no alteration of the V4 region. Thirteen total nucleotide changes were found; only two clones demonstrated more than one change, and nine clones contained only one change. One of these changes was a nucleotide deletion, and nine changes resulted in amino acid substitutions (Fig. 2B). The majority of these changes occurred in the V4 hypervariable region. Slightly more than half (7 of 12) of the nucleotide changes were detected in clones derived from one implant, 11-8. Only one nucleotide change was observed more than once (nt 7430; A→G).

One implant (11-8) was also analyzed for viral sequences at 9 weeks p.i. Of the six clones analyzed, three contained no changes, and of the remaining three clones, each contained two nucleotide changes. Four of these two-nucleotide changes were silent mutations (data not shown). The two nucleotide substitutions that resulted in amino acid changes were within the same clone. None of the changes were similar between clones. To ensure that observed changes were not due solely to technical manipulations, 11 clones of HIV-1_{JR-CSF} and eight clones derived from HIV-1_{NL4-3} plasmid DNA were amplified, cloned, and sequenced in parallel with the experimental samples. No nucleotide changes were observed (data not shown). These results demonstrate that little genetic variation of the V4 loop or CD4-binding domain occurred during the 6 weeks of infection. Although most of the sequence variation occurred in HIV-1_{NL4-3}-infected implants, the pattern of variation is consistent with random mutations rather than mutations which appear following selective pressure. Of the 11 variant genotypes observed, none is represented more than once. In addition, the frequency of observed silent mutations (23%) is consistent with the frequency of random mutations and is not

TABLE 2. Viral burden in HIV-1_{JR-CSF}- and HIV-1_{NL4-3}-infected implants[a]

Wk p.i.	Copies of HIV genome/10^5 cells			Copies of HIV genome/10^5 $CD4^+$ cells		
	HIV-1_{NL4-3}	HIV-1_{JR-CSF}	Approx fold difference	HIV-1_{NL4-3}	HIV-1_{JR-CSF}	Approx fold difference
3	13,100	1,100	11	16,400	1,500	11
4–6	13,200	2,800	5	378,400	3,350	112

[a] HIV-1-infected implants were analyzed as described in the legend to Fig. 1. Values are the averages for the implants depicted in Fig. 1. Fold difference indicates the difference in viral burden between HIV-1_{NL4-3} and HIV-1_{JR-CSF} at the indicated time points.

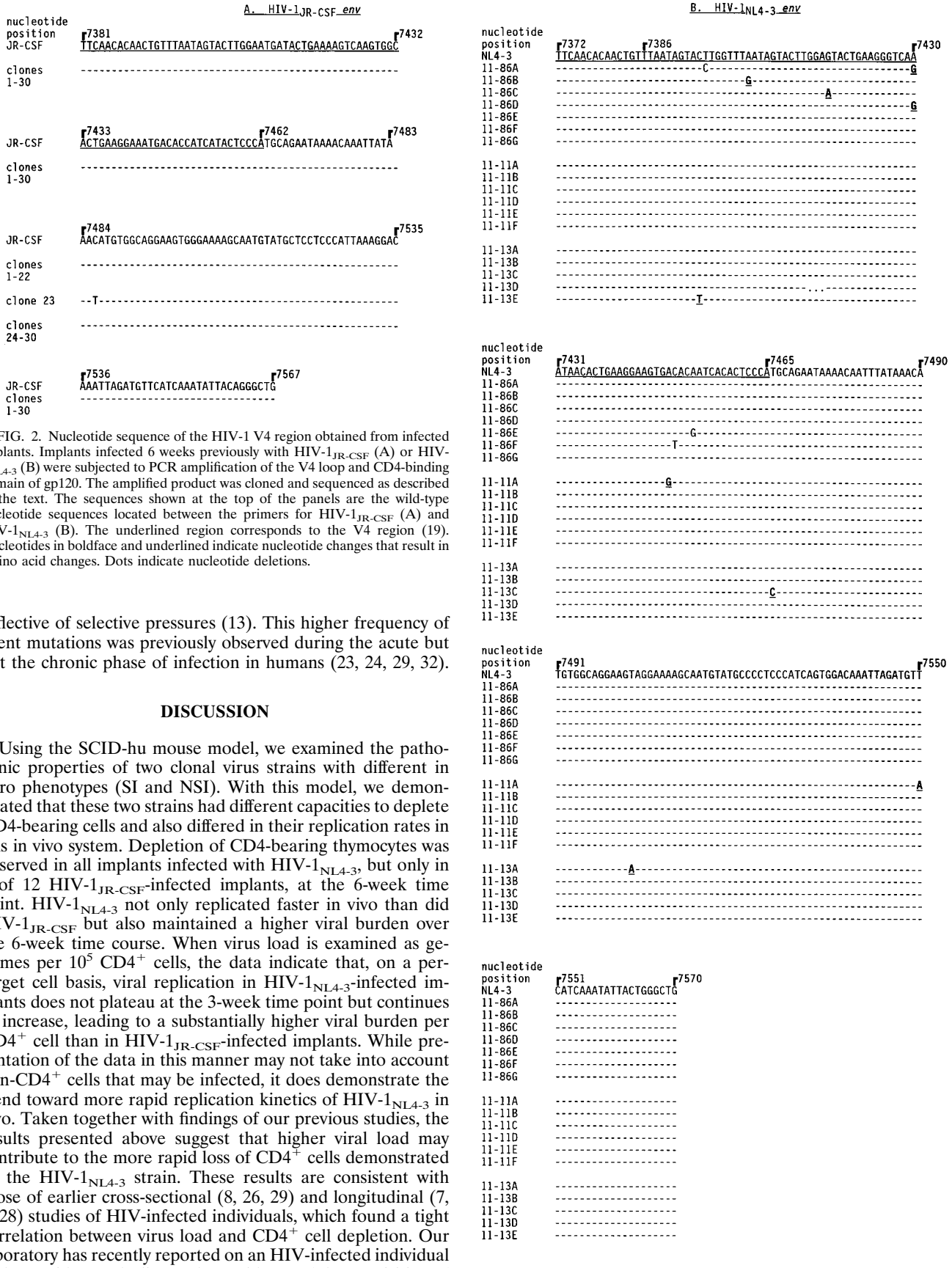

FIG. 2. Nucleotide sequence of the HIV-1 V4 region obtained from infected implants. Implants infected 6 weeks previously with HIV-1_{JR-CSF} (A) or HIV-1_{NL4-3} (B) were subjected to PCR amplification of the V4 loop and CD4-binding domain of gp120. The amplified product was cloned and sequenced as described in the text. The sequences shown at the top of the panels are the wild-type nucleotide sequences located between the primers for HIV-1_{JR-CSF} (A) and HIV-1_{NL4-3} (B). The underlined region corresponds to the V4 region (19). Nucleotides in boldface and underlined indicate nucleotide changes that result in amino acid changes. Dots indicate nucleotide deletions.

reflective of selective pressures (13). This higher frequency of silent mutations was previously observed during the acute but not the chronic phase of infection in humans (23, 24, 29, 32).

DISCUSSION

Using the SCID-hu mouse model, we examined the pathogenic properties of two clonal virus strains with different in vitro phenotypes (SI and NSI). With this model, we demonstrated that these two strains had different capacities to deplete CD4-bearing cells and also differed in their replication rates in this in vivo system. Depletion of CD4-bearing thymocytes was observed in all implants infected with HIV-1_{NL4-3}, but only in 2 of 12 HIV-1_{JR-CSF}-infected implants, at the 6-week time point. HIV-1_{NL4-3} not only replicated faster in vivo than did HIV-1_{JR-CSF} but also maintained a higher viral burden over the 6-week time course. When virus load is examined as genomes per 10^5 $CD4^+$ cells, the data indicate that, on a per-target cell basis, viral replication in HIV-1_{NL4-3}-infected implants does not plateau at the 3-week time point but continues to increase, leading to a substantially higher viral burden per $CD4^+$ cell than in HIV-1_{JR-CSF}-infected implants. While presentation of the data in this manner may not take into account non-$CD4^+$ cells that may be infected, it does demonstrate the trend toward more rapid replication kinetics of HIV-1_{NL4-3} in vivo. Taken together with findings of our previous studies, the results presented above suggest that higher viral load may contribute to the more rapid loss of $CD4^+$ cells demonstrated by the HIV-1_{NL4-3} strain. These results are consistent with those of earlier cross-sectional (8, 26, 29) and longitudinal (7, 9, 28) studies of HIV-infected individuals, which found a tight correlation between virus load and $CD4^+$ cell depletion. Our laboratory has recently reported on an HIV-infected individual with a rapid CD4 decline and no evidence of the acquisition of

SI isolates. Rather, there was an increase in viral load coincident with the onset of $CD4^+$ T-cell depletion (9). Thus, in humans, while viral phenotype may influence disease progression, it appears than an increase in viral load can influence the progression of disease. The SCID-hu mouse model should prove useful in modeling these events and investigating therapeutic strategies.

It is possible that the SI phenotype exhibited by the HIV-1_{NL4-3} strain allows for more efficient viral spread, resulting in higher viral burden. While the current study did not address this question, it was recently shown that in the SCID-hu mouse model, both primary and cloned SI isolates are more pathogenic than NSI isolates (5a, 15, 16). While identical virus strains were not tested, these results appear to be in contrast to what has been observed in the hu-PBL-SCID model (21), in which NSI isolates are more pathogenic. Interestingly, Kollmann et al. (16) showed that the HIV-1_{SF162} isolate is relatively nonpathogenic in the SCID-hu mouse, whereas Mosier et al. (21) found it to be cytopathic in hu-PBL-SCID mice. This apparent difference may be due to different types and activation states of the human cells used to reconstitute these two murine systems.

While minimal depletion was seen at 6 weeks p.i. in implants infected with 100 IU of HIV-1_{JR-CSF}, depletion has been previously observed by this time point when 10^3 IU was used (2). The minimal depletion observed in HIV-1_{JR-CSF}-infected implants with the smaller inoculum used in this study suggests that the relationship between virus load and $CD4^+$ cell number is a dynamic interaction. Because thymopoiesis is a self-renewing source of new T cells, replacement of $CD4^+$ thymocytes may occur efficiently enough to replace cells lost to the virus when viral replication is slow. However, a virus with faster replication kinetics may disrupt this equilibrium, resulting in the severe loss of $CD4^+$ cells, as observed in HIV-1_{NL4-3}-infected implants. Additional studies in our laboratory, which examined the pathogenic capacity of accessory gene mutants of HIV-1, demonstrated that those mutants that are replication attenuated are also attenuated for pathogenicity (3, 12). Taken together, our results suggest that replication kinetics and pathogenicity are closely tied and that this may be due to a balance between $CD4^+$ cell infection and loss and the generation of new cells. This inference is consistent with the elegant studies of Wei et al. (31) and Ho et al. (11), which showed that the immune system replaces approximately 2×10^9 T cells per day, in an attempt to maintain the balance between $CD4^+$ T-cell infection and loss and T-cell replacement in the periphery. In an HIV-1-infected individual, faster viral replication would result in more rapid loss of $CD4^+$ T cells both from the periphery and from the lymphoid organs. The mechanisms of cell replacement (i.e., proliferation of mature T cells and differentiation of T cells from hematopoietic precursors) are unable to operate rapidly enough, leaving the host with a net deficit of $CD4^+$ cells. Our results support the hypothesis that management of viral burden may provide therapeutic benefit to HIV-1-infected individuals by delaying disease onset.

Little sequence variation was found in HIV-1_{JR-CSF} isolated from implants 6 weeks p.i., similar to what is observed after amplification of the DNA corresponding to the V4 region during acute retroviral syndrome in humans (23). Although HIV-1 exhibits extensive genetic variation within an individual during the chronic phase of disease, little or no sequence variation is observed prior to seroconversion during the early phase of the acute infection (23, 33). This lack of extensive variation is thought to reflect the lack of immune system-mediated selection. It is unlikely that either a human- or mouse-derived immune response is generated within the Thy/Liv implant of the SCID-hu mouse. Therefore, the lack of genetic variation observed in HIV-1_{JR-CSF}-infected implants probably reflects the absence of immune system-mediated selective pressure. The greater sequence variation exhibited by HIV-1_{NL4-3} than by HIV-1_{JR-CSF} most likely reflects the greater number of replication cycles required to reach the higher viral burden observed in HIV-1_{NL4-3}-infected implants (Fig. 1 and Table 2). Taken together, our results indicate that the viral variation observed in the SCID-hu mouse model reflects the acute rather than the chronic phase of HIV-1 infection of humans, and the SCID-hu mouse may therefore serve as a useful model for addressing questions of early HIV-1 infection and disease and in the testing of early therapeutic strategies.

ACKNOWLEDGMENTS

We thank Lianying Gao and Greg Bristol for excellent technical assistance and Wendy Aft for preparation of the manuscript.

This work was supported by the UCLA Center for AIDS Research (NIH AI28697), NIH grant AI36059, and the McCarthy Family Foundation. G.M.A. is a Pediatric AIDS Foundation Scholar.

REFERENCES

1. **Adachi, A., H. E. Gendelman, S. Koenig, T. Folks, R. Willey, A. Rabson, and M. A. Martin.** 1986. Production of acquired immunodeficiency syndrome-associated retrovirus in human and nonhuman cells transfected with an infectious molecular clone. J. Virol. **59:**284–291.
2. **Aldrovandi, G. M., G. Feuer, L. Gao, B. Jamieson, M. Kristeva, I. S. Y. Chen, and J. A. Zack.** 1993. The SCID-hu mouse as a model for HIV-1 infection. Nature (London) **363:**732–736.
3. **Aldrovandi, G. M., and J. A. Zack.** Replication and pathogenicity of HIV-1 accessory gene mutants in SCID-hu mice. Submitted for publication.
4. **Bonyhadi, M. L., L. Rabin, S. Salimi, D. A. Brown, J. Kosek, J. M. McCune, and H. Kaneshima.** 1993. HIV induces thymus depletion *in vivo*. Nature (London) **363:**728–736.
5. **Bosma, G. C., R. P. Custer, and M. J. Bosma.** 1983. A severe combined immunodeficiency mutation in the mouse. Nature (London) **301:**527–530.

5a. **Camerini, D., J. Zack, and I. S. Y. Chen.** Unpublished observations.

6. **Cann, A. J., Y. Koyanagi, and I. S. Y. Chen.** 1988. High efficiency transfection of primary human lymphocytes and studies of gene expression. Oncogene **3:**123–128.
7. **Connor, R. I., H. Mohri, Y. Cao, and D. D. Ho.** 1993. Increased viral burden and cytopathicity correlate temporally with $CD4^+$ T-lymphocyte decline and clinical progression in human immunodeficiency type 1-infected individuals. J. Virol. **67:**1772–1777.
8. **Coombs, R. W., A. C. Collier, J.-P. Allain, B. Nikora, M. Leuther, G. F. Gjerset, and L. Corey.** 1989. Plasma viremia in human immunodeficiency virus infection. N. Engl. J. Med. **321:**1626–1631.
9. **Daar, E. S., T. Chernyavskiy, J.-Q. Zhao, P. Krogstad, I. S. Y. Chen, and J. A. Zack.** 1995. Sequential determination of viral load and phenotype in human immunodeficiency virus type 1 infection. AIDS Res. Hum. Retroviruses **11:**3–9.
10. **Ho, D. D., T. Moudgil, and M. Alam.** 1989. Quantitation of human immunodeficiency virus type 1 in the blood of infected persons. N. Engl. J. Med. **321:**1621–1625.
11. **Ho, D. D., A. U. Neumann, A. S. Perelson, W. Chen, J. M. Leonard, and M. Markowitz.** 1995. Rapid turnover of plasma virions and CD4 lymphocytes in HIV-1 infection. Nature (London) **373:**123–126.
12. **Jamieson, B. D., G. M. Aldrovandi, V. Planelles, J. B. M. Jowett, L. Gao, L. M. Bloch, I. S. Y. Chen, and J. A. Zack.** 1994. Requirement of human immunodeficiency virus type 1 *nef* for in vivo replication and pathogenicity. J. Virol. **61:**3478–3485.
13. **Jukes, T. H., and J. L. King.** 1979. Evolutionary nucleotide replacements in DNA. Nature (London) **281:**605–606.
14. **Jurriaans, S., B. Van Gemen, G. J. Weverling, D. Van Strijp, P. Nara, R. Coutinho, M. Koot, H. Schuitemaker, and J. Goudsmit.** 1994. The natural history of HIV-1 infection: virus load and virus phenotype independent determinants of clinical course? Virology **204:**223–233.
15. **Kaneshima, H., L. Su, M. L. Bonyhadi, R. I. Connor, D. D. Ho, and J. M. McCune.** 1994. Rapid-high, syncytium-inducing isolates of human immunodeficiency virus type 1 induce cytopathicity in the human thymus of the SCID-hu mouse. J. Virol. **68:**8188–8192.
16. **Kollmann, T. R., A. Kim, M. Pettoello-Mantovani, M. Hachamovitch, A. Rubinstein, M. M. Goldstein, and H. Goldstein.** 1995. Divergent effects of

chronic HIV-1 infection on human thymocyte maturation in SCID-hu mice. J. Immunol. **154:**907–921.
17. **Koyanagi, Y., S. Miles, R. T. Mitsuyasu, J. E. Merrill, H. V. Vinters, and I. S. Y. Chen.** 1987. Dual infection of the central nervous system by AIDS viruses with distinct cellular tropisms. Science **236:**819–822.
18. **Lawn, R. M., A. Efstratindus, C. O'Connell, and T. Maniatis.** 1980. The nucleotide sequence of the human β-globin gene. Cell **21:**647–651.
19. **Leonard, K. L., W. M. Spellman, L. Riddle, R. J. Harris, J. N. Thomas, and T. J. Gregory.** 1990. Assignment of intrachain disulfide bonds and characterization of potential glycosylation sites of the type 1 recombinant human immunodeficiency virus envelope glycoprotein (gp120) expressed in Chinese hamster ovary cells. J. Biol. Chem. **265:**10373–10382.
20. **McCune, J. M., R. Namikawa, H. Kaneshima, L. D. Shultz, M. Lieberman, and I. L. Weissman.** 1988. The SCID-hu mouse: murine model for the analysis of human hematolymphoid differentiation and function. Science **241:**1632–1639.
21. **Mosier, D. E., R. J. Gulizia, P. D. MacIsaac, B. E. Torbett, and J. A. Levy.** 1993. Rapid loss of $CD4^+$ T cells in human-PBL-SCID mice by noncytopathic HIV isolates. Science **260:**689–692.
22. **Namikawa, R., K. N. Weilbaecter, H. Kareshima, E. Yee, and J. M. McCune.** 1990. Long term human hematopoiesis in the SCID-hu mouse. J. Exp. Med. **172:**1055–1063.
23. **Pang, S., Y. Shlesinger, E. S. Daar, T. Moudgil, D. D. Ho, and I. S. Y. Chen.** 1992. Rapid generation of sequence variation during primary HIV-1 infection. AIDS **6:**453–460.
24. **Pang, S., H. V. Vinters, T. Akashi, W. A. O'Brien, and I. S. Y. Chen.** 1991. HIV-1 Env sequence variation in brain tissue of patients with AIDS encephalopathy. J. Acquired Immune Defic. Syndr. **4:**1082–1092.
25. **Piatak, M., M. S. Saag, L. C. Yang, S. J. Clark, J. C. Kapper, K. C. Luk, B. H. Hahn, G. M. Shaw, and J. D. Lifson.** 1993. High levels of HIV-1 in plasma during all stages of infection determined by competitive PCR. Science **259:** 1749–1754.
26. **Saag, M. S., M. J. Crain, W. D. Decker, S. Campbell-Hill, S. Robinson, W. E. Brown, M. Leuther, R. J. Whitley, B. H. Hahn, and G. M. Shaw.** 1991. High-level viremia in adults and children infected with human immunodeficiency virus: relation to disease stage and $CD4^+$ lymphocyte levels. J. Infect. Dis. **164:**72–80.
27. **Sanger, F., S. Nicklen, and A. R. Coulson.** 1977. DNA sequencing with chain-terminating inhibitors. Proc. Natl. Acad. Sci. USA **74:**5463–5467.
28. **Schnittman, S. M., J. J. Greenhouse, M. C. Psallidopoulos, M. Baseler, N. P. Salzman, A. S. Fauci, and H. C. Lane.** 1990. Increasing viral burden in CD4+ T cells from patients with human immunodeficiency virus (HIV) infection reflects rapidly progressive immunosuppression and clinical disease. Ann. Intern. Med. **113:**438–443.
29. **Simmonds, P., P. Balfe, C. A. Ludlam, J. O. Bishop, and A. J. L. Brown.** 1990. Analysis of sequence diversity of hypervariable regions of the external glycoprotein of human immunodeficiency virus type 1. J. Virol. **64:**5840–5850.
30. **Stanley, S. K., J. M. McCune, H. Kaneshima, J. S. Justement, M. Sullivan, E. Boone, M. Baseler, J. Adelsberger, M. Bonyhadi, J. Orenstein, C. H. Fox, and A. S. Fauci.** 1993. Human immunodeficiency virus infection of the human thymus and disruption of the thymic microenvironment in the SCID-hu mouse. J. Exp. Med. **178:**1151–1163.
31. **Wei, X., S. K. Ghosh, M. E. Taylor, V. A. Johnson, E. A. Emini, P. Deutsch, J. D. Lifson, S. Bonhoeffer, M. A. Nowak, B. H. Hahn, M. S. Saag, and G. M. Shaw.** 1995. Viral dynamics in human immunodeficiency virus type 1 infection. Nature (London) **373:**117–122.
32. **Wolfs, T. F. W., G. Zwart, M. Bakker, M. Valk, C. L. Kuiken, and J. Goudsmit.** 1991. Naturally occurring mutations within HIV-1 V3 genomic RNA lead to antigenic variation dependent on a single amino acid substitution. Virology **185:**195–205.
33. **Wolinsky, S. M., C. M. Wike, B. T. M. Korber, C. Hutto, W. P. Parks, L. L. Rosenblum, K. J. Kunstman, M. R. Furtado, and J. L. Munoz.** 1990. Selective transmission of human immunodeficiency virus type-1 variants from mothers to infants. Science **255:**1134–1136.
34. **Zack, J. A., S. J. Arrigo, S. R. Weitsman, A. S. Go, A. Haislip, and I. S. Y. Chen.** 1990. HIV-1 entry into quiescent primary lymphocytes: molecular analysis reveals a labile, latent viral structure. Cell **61:**213–222.
35. **Zack, J. A., A. M. Haislip, P. Krogstad, and I. S. Y. Chen.** 1992. Incompletely reverse transcribed human immunodeficiency virus type 1 genomes in quiescent cells can function as intermediates in the virus life cycle. J. Virol. **66:**1717–1725.